Identification of Residues Involved in the Interaction of *Staphylococcus aureus* Fibronectin-Binding Protein with the $^{4}F1^{5}F1$ Module Pair of Human Fibronectin Using Heteronuclear NMR Spectroscopy†

Christopher J. Penkett,‡ Christopher M. Dobson,‡ Lorna J. Smith,‡ Jeremy R. Bright,§ Andrew R. Pickford,§ Iain D. Campbell,‡,§ and Jennifer R. Potts*,§

Department of Biochemistry, University of Oxford, South Parks Road, Oxford OX1 3QU, and Oxford Centre for Molecular Sciences, New Chemistry Laboratory, University of Oxford, South Parks Road, Oxford OX1 3QT, U.K.

Received September 29, 1999; Revised Manuscript Received December 23, 1999

ABSTRACT: Many pathogenic Gram-positive bacteria express cell surface proteins that bind to components of the extracellular matrix. This paper describes studies of the interaction between ligand binding repeats (D3 and D1−D4) of a fibronectin-binding protein from *Staphylococcus aureus* with a module pair ($^{4}F1^{5}F1$) from the N-terminal region of fibronectin. When D3 was added to isotope-labeled $^{4}F1^{5}F1$, ^{1}H, ^{15}N, and ^{13}C NMR chemical shift changes indicate that binding is primarily via residues in $^{4}F1$, although a few residues in $^{5}F1$ are also affected. Both hydrophobic and electrostatic interactions appear to be involved. The NMR data indicate that part of the D3 repeat converts from a disordered to a more ordered, extended conformation on binding to $^{4}F1^{5}F1$. In further NMR experiments, selective reduction of the intensity of D1−D4 resonances was observed on binding to $^{4}F1^{5}F1$, consistent with previous suggestions that in each of D1, D2, and D3 repeats, the main fibronectin binding site is in the C-terminal region of the repeat. In D1−D4, these regions also appear to go from a disordered to a more ordered conformation of fibronectin binding. Although the regions of the two proteins which interact had been previously identified, the findings presented here identify, for the first time, the specific residues in both proteins that are likely to be involved in the interaction.

Many pathogenic microorganisms use cell surface adhesins to target extracellular matrix (ECM)[1] macromolecules as an initial step for invading host cells (*1*, *2*). The acronym MSCRAMM (microbial surface components recognizing adhesive matrix molecules) has been used to describe this family of microbial adhesins. The first ECM protein shown to act as a substrate for microbial adhesion was fibronectin (*3*). Each fibronectin monomer is composed of three different types of protein modules (F1−F3), which have also been found in a variety of other proteins (*4*).

Fibronectin-binding proteins from a number of different Gram-positive bacteria have a similar structural organization, with the primary fibronectin binding site consisting of three to five repeats, each 40−50 residues in length. This ligand binding region of fibronectin-binding protein FnBPA from *Staphylococcus aureus* consists of three full-length repeats (D1−D3) and a shorter repeat (D4). The domain in fibronectin which is primarily recognized by the microbial fibronectin-binding repeats is located at the N-terminus of the molecule (*5*) which contains five F1 ($^{1-5}F1$) modules. Additional binding sites for *S. aureus* are located in the C-terminal portion of fibronectin (*6*, *7*). Synthetic peptides of D1, D2, and D3 bind $^{1-5}F1$ from fibronectin (*8*). The primary binding site is in $^{4}F1^{5}F1$, the same fibronectin module pair that noncovalently binds to fibrin (*9*, *10*). However, neither $^{4}F1$ nor $^{5}F1$ has been shown to bind fibrin (*9*) or D1−D4 (*8*) as single modules.

Much of the binding activity of the D repeats appears to be mediated through their C-terminal halves (*8*, *11*). In these regions, D1 and D2 are very similar to each other in sequence. In contrast, D3 is quite different in this region (*11*, *12*) and binds with a higher affinity (*8*). A synthetic peptide, encompassing residues 17−37 of D3 ($D3_{17-37}$), has been shown to have a binding affinity for fibronectin similar to that of a larger peptide ($D3_{2-38}$). Reduction of the number of residues from either the N- or C-termini of $D3_{17-37}$ results in peptides with greatly diminished activity (*11*). Sequence analyses and binding studies using synthetic domains of fibronectin-binding repeats from *S. aureus* and *Streptococcus dysgalactiae* have identified conserved acidic, hydrophobic, and glycine residues that appear to be important for ligand

† This research was supported by the Wellcome Trust, the Biotechnology and Biological Sciences Research Council, the Medical Research Council, and the Engineering and Physical Sciences Research Council. This is a contribution from the Oxford Centre for Molecular Sciences. J.R.P., A.R.P., and J.R.B. thank the Wellcome Trust for financial support. L.J.S. is a Royal Society University Research Fellow.

* To whom correspondence should be addressed: Department of Biochemistry, University of Oxford, South Parks Road, Oxford OX1 3QU, U.K. E-mail: jenp@bioch.ox.ac.uk.

‡ Oxford Centre for Molecular Sciences, New Chemistry Laboratory, University of Oxford.

§ Department of Biochemistry, University of Oxford.

[1] Abbreviations: ECM, extracellular matrix; ESMS, electrospray mass spectrometry; HPLC, high-performance liquid chromatography; HSQC, heteronuclear single-quantum correlation; MSCRAMM, microbial surface components recognizing adhesive matrix molecules; NMR, nuclear magnetic resonance; NOESY, nuclear Overhauser effect spectroscopy; TOCSY, total correlation spectroscopy.

10.1021/bi992267k CCC: $19.00
Published on Web 02/26/2000

binding (*11*, *13*). A considerable degree of cross-reactivity has been identified between synthetic repeats from different Gram-positive bacteria; for example, the A2 repeat from *St. dysgalactiae* inhibits binding of *S. aureus* to fibronectin and $^{1-5}$F1 (*13*, *14*).

Both modules in the structure of ^{4}F1^{5}F1 have the consensus F1 fold of a double-stranded antiparallel β-sheet folded over a triple-stranded β-sheet (*10*). The two modules form an elongated structure, with the interface between the modules resulting in a relatively well-defined intermodule orientation. This interface between the two modules is not conserved in ^{1}F1^{2}F1 (the only other F1F1 structure available; *15*).

Recently, it was shown that D1−D4 from *S. aureus* exist in a highly unfolded state under physiological conditions (*12*, *16*, *17*). Studies using circular dichroism (CD) spectroscopy suggest that, on binding to the N-terminal domain of fibronectin, at least part of the D1−D4 sequence adopts a more ordered, extended conformation (*16*). Although CD provides evidence for this conformation change on binding, detailed interpretation of the CD spectra for systems in which there are protein−protein interactions can be difficult as the signals from the different species overlap. Here, therefore, we use NMR spectroscopy to study the two interacting proteins separately by using ^{15}N- and ^{13}C-labeling techniques combined with either isotope editing or isotope filtering in the pulse sequences, so that signals from just the labeled or unlabeled protein can be observed. This paper describes NMR studies designed to identify binding sites in both ^{4}F1^{5}F1 and D1−D4 and to investigate structural changes that may occur when the proteins associate.

MATERIALS AND METHODS

Sample Preparation. Uniformly ^{15}N-labeled D1−D4 ([*u*-^{15}N]D1−D4) from FnBP type C from *S. aureus* was produced as previously described (*12*). D3$_{17-37}$ and D3$_{7-38}$ (residues 837−857 and 827−858, respectively, from FnBPA from *S. aureus*) were synthesized using standard Fmoc methodology on an Applied Biosystems 430A peptide synthesizer and were purified by reverse phase high-performance liquid chromatography (HPLC). The purified peptides were checked for purity and correct molecular mass by electrospray mass spectrometry (ESMS). ^{4}F1^{5}F1 (residues 152−244 of mature human fibronectin) was expressed in either *Saccharomyces cerevisiae* or *Pichia pastoris* as described below. Uniformly ^{15}N-labeled ^{4}F1^{5}F1 ([*u*-^{15}N]^{4}F1^{5}F1), for the experiments with D3$_{17-37}$, was expressed in *Sa. cerevisiae* and purified as previously described (*18*, *19*). Unlabeled ^{4}F1^{5}F1 was expressed in *P. pastoris* using procedures analogous to those described previously (*20*), and further, [*u*-^{15}N]^{4}F1^{5}F1 and uniformly ^{13}C- and ^{15}N-labeled ^{4}F1^{5}F1 ([*u*-^{13}C,^{15}N]^{4}F1^{5}F1) were expressed in *P. pastoris* as described elsewhere (*21*). ^{4}F1^{5}F1 expressed in *P. pastoris* was purified by cation exchange chromatography and reverse phase HPLC (*15*). The purity and identity of ^{4}F1^{5}F1 (labeled and unlabeled) were confirmed by ESMS.

NMR Spectroscopy. NMR samples were prepared in 90% H_2O/10% D_2O, and the pH was then adjusted to the stated values with small quantities of sodium hydroxide (1 M) and hydrochloric acid (1 M) solutions. All the NMR experiments were performed on spectrometers belonging to the Oxford Centre for Molecular Sciences (OCMS) with ^{1}H operating frequencies of 500, 600, and 750 MHz. The spectrometers are all equipped with Oxford Instruments superconducting magnets, OMEGA software and digital control equipment (Bruker Instruments), home-built triple-resonance pulsed-field-gradient probe heads (*22*), and home-built linear amplifiers for ^{1}H, ^{15}N, and ^{13}C nuclei. Spectra were recorded at 37 °C unless otherwise stated.

Interaction of D3 with ^{4}F1^{5}F1. Small aliquots of D3$_{17-37}$ (∼4 mM, pH 6.5) were added to [*u*-^{15}N]^{4}F1^{5}F1 (∼0.3 mM, pH 5.5), and the pH was adjusted to 5.5. After each addition of peptide, a two-dimensional ^{15}N−^{1}H HSQC (*23*) spectrum was recorded. At the final ^{4}F1^{5}F1:D3$_{17-37}$ ratio (∼1:8), two-dimensional ^{15}N-decoupled NOESY (*24*−*26*), three-dimensional NOESY-HSQC (*27*−*29*), and two-dimensional ^{15}N-filtered (*30*) TOCSY and NOESY experiments were performed. For the ^{15}N-decoupled NOESY and ^{15}N-filtered NOESY and TOCSY spectra, we used a gradient echo technique (*31*) for suppressing the strong solvent resonance without the need for presaturation; the ^{15}N-filtered experiments were conducted at 23 °C. The ^{15}N-filtered experiments were recorded with alternate FIDs (free induction decays) stored in different memory locations for later manipulation during processing. These experiments were processed in two different ways. First, the alternate FIDs were subtracted so that the final NMR spectrum shows cross-peaks from protons directly attached to ^{15}N nuclei in F_2; the second method adds alternately saved FIDs and shows cross-peaks from protons that are not directly attached to ^{15}N nuclei in F_2. ^{1}H and ^{15}N chemical shift assignments for ^{4}F1^{5}F1 at pH 5.5 were obtained using assignments at pH 4.5 (*18*, *32*) and from ^{15}N−^{1}H HSQC spectra acquired at pH 4.5, 5.0, and 5.5.

To determine changes in methyl group chemical shifts, aliquots of D3$_{7-38}$ (1.8 mM, pH 5.4) were lyophilized and added to [*u*-^{13}C^{15}N]^{4}F1^{5}F1 (0.5 mM, pH 5.3) up to a final ^{4}F1^{5}F1:D3$_{17-38}$ ratio of ∼1:4. After each addition of peptide, the pH was adjusted to 5.3 and a two-dimensional ^{13}C−^{1}H CT-HSQC (*33*, *34*) spectrum was acquired. In addition, a three-dimensional ^{13}C−^{1}H NOESY-HSQC spectrum of [^{13}C^{15}N]^{4}F1^{5}F1 and three-dimensional CBCA(CO)NH (*35*) and three-dimensional HCC(CO)NH-TOCSY (*36*) spectra of [*u*-^{13}C^{15}N]^{4}F1^{5}F1 and [*u*-^{13}C^{15}N]^{4}F1^{5}F1/D3$_{7-38}$ were acquired to aid the assignment of ^{13}CH$_3$ resonances.

To compare changes in D3 residue peak intensities upon binding to ^{4}F1^{5}F1, aliquots of D3$_{7-38}$ (1.3 mM, pH 5.3) were lyophilized and added to [*u*-^{15}N]^{4}F1^{5}F1 (1.2 mM, pH 5.3). ^{15}N-filtered TOCSY spectra were acquired at D3$_{7-38}$:^{4}F1^{5}F1 ratios of ∼1:0.3, 1:0.5, and 1:1 at 37 °C. Spectra were processed so that only resonances arising from the unlabeled D3$_{7-38}$ were observed and the intensities of H^{N}−H^{α} cross-peaks were measured.

Interaction of [u-^{15}N]D1−D4 with ^{4}F1^{5}F1. Aliquots of unlabeled ^{4}F1^{5}F1 (∼2 mM, pH 5.4) were added to [*u*-^{15}N]-D1−D4 (∼0.6 mM, pH 5.5), and the pH was adjusted to 5.5. ^{15}N−^{1}H HSQC spectra were recorded for ^{15}N-labeled material at D1−D4:^{4}F1^{5}F1 ratios of approximately 1:0, 1:0.7, and 1:1.4.

RESULTS AND DISCUSSION

Changes to D3$_{17-37}$. NMR spectra of large protein complexes are complicated by overlap of resonances and broad lines due to long correlation times. The main binding

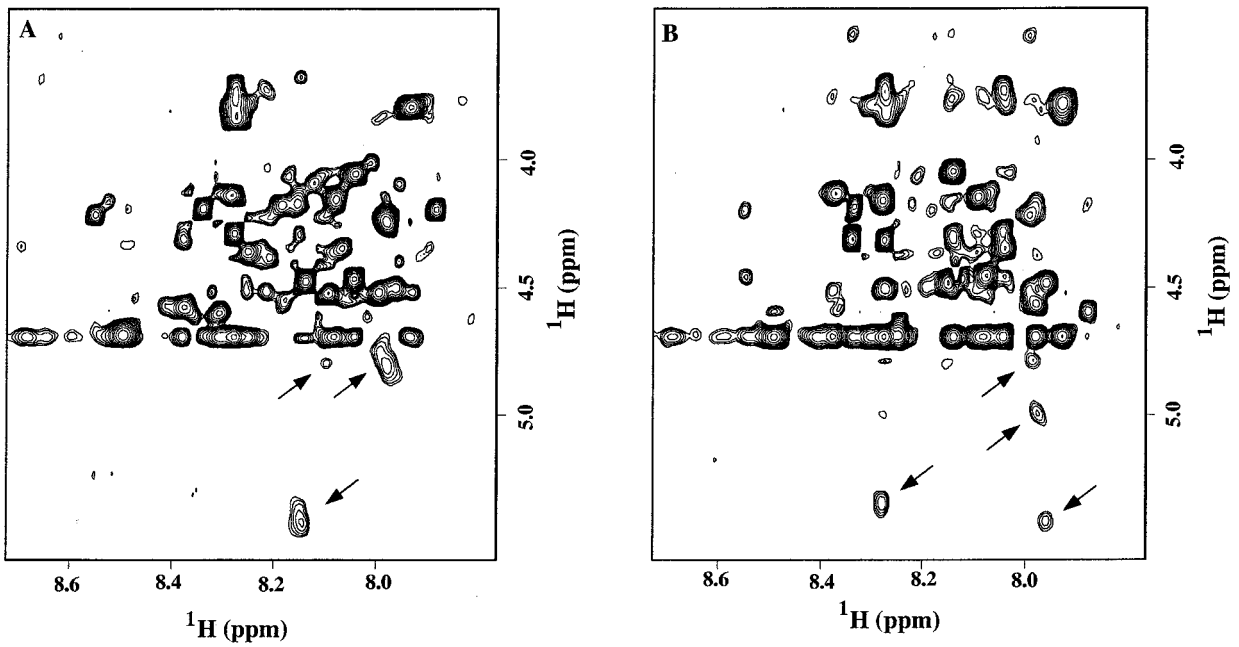

FIGURE 1: Fingerprint region of two-dimensional ^{15}N-filtered (A) TOCSY and (B) NOESY spectra (recorded at a ^{1}H frequency of 750 MHz) of $D3_{17-37}$ in the presence of [*u*-^{15}N]$^4F1^5F1$ at pH 5.5 and 23 °C and at a $^4F1^5F1$:$D3_{17-37}$ ratio of ~1:8. The resonances of $^4F1^5F1$ were eliminated using isotope filtering. The indicated peaks appear at higher chemical shift than peaks in spectra of uncomplexed $D3_{17-37}$.

site in fibronectin for D1−D4 of FnBPA of *S. aureus* is in the $^4F1^5F1$ module pair (*8*, *14*), and of the D repeats, D3 binds with the highest affinity, primarily via residues in the C-terminal region of the repeat (*8*, *11*). Thus, to minimize the molecular weight of the complex, $^4F1^5F1$ and $D3_{17-37}$ were used.

By using [*u*-^{15}N]$^4F1^5F1$, the changes to cross-peaks in unlabeled $D3_{17-37}$ can be monitored by filtering out the peaks arising from the ^{15}N-labeled protein using the ^{15}N-filtered TOCSY and NOESY experiments that are described in Materials and Methods. Figure 1 shows the fingerprint regions of ^{15}N-filtered TOCSY and NOESY spectra of $D3_{17-37}$ in the presence of [*u*-^{15}N]$^4F1^5F1$. Cross-peaks indicated by arrows can be seen at chemical shifts of 4.7−5.5 ppm in the H^α dimension of both spectra. Free $D3_{17-37}$ has no H^α chemical shifts greater than 4.7 ppm, and thus, the resonances in the TOCSY spectrum arise from H^α groups of $D3_{17-37}$ residues that undergo a change in chemical shift on binding to $^4F1^5F1$. These downfield-shifted H^α chemical shifts in $D3_{17-37}$ strongly indicate that some residues in $D3_{17-37}$ adopt extended conformations in the complex with $^4F1^5F1$ (*37*). This is particularly significant as residues in the C-terminal region of D3 have been identified as having a preference for adopting β rather than α main chain ϕ and ψ conformations in the unfolded state (*12*). Hence, this preferred conformation may be selected out of the disordered ensemble on binding to fibronectin. It is important to note that large chemical shift changes can also occur as a result of the proximity of aromatic groups; only the determination of the three-dimensional structure of the complex will allow this possibility to be eliminated. The cross-peaks in this region of the NOESY spectrum (indicated in Figure 1B) are not present in the NOESY spectrum of free $D3_{17-37}$ and may be either NOEs between protons in the bound peptide or NOEs between the peptide and $^4F1^5F1$.

Mapping the D3 Binding Site on $^4F1^5F1$. Small amounts of $D3_{17-37}$ were added to [*u*-^{15}N]$^4F1^5F1$ for a number of additions of peptide, and two-dimensional ^{15}N−^{1}H HSQC spectra were recorded. Figure 2 shows an overlay of a region of the HSQC spectra at various $D3_{17-37}$ concentrations. In Figure 2, the chemical shifts of some cross-peaks (for example, Gly10 and Gly71) are essentially unaltered by addition of the peptide, while large chemical shift changes are observed for a number of residues (for example, Gly37 and Gly80). To reassign significantly shifted peaks and to obtain complete ^{1}H resonance assignments, a three-dimensional NOESY-HSQC experiment was performed at a $^4F1^5F1$:$D3_{17-37}$ ratio of ~1:8. The ^{1}H and ^{15}N resonance assignments of the free and D3-complexed $^4F1^5F1$ module pair could then be compared. Differences in the backbone (^{15}N, H^N, and H^α) chemical shifts between the free and bound forms of $^4F1^5F1$ are shown in Figure 3; the magnitude of the (scaled) combined changes to ^{15}N and H^N chemical shifts are also shown in Figure 3A. Residues in both $^4F1$ and $^5F1$ exhibit chemical shift changes between the free and peptide-bound forms of $^4F1^5F1$, although the majority of changes occur in $^4F1$. The fact that chemical shift changes occur in both modules is consistent with a previous study which indicated that the module pair was required for binding to D1−D4 (*8*).

In Figure 4, the combined changes to ^{15}N and H^N chemical shifts (Figure 3A) have been mapped onto the previously determined structure of uncomplexed $^4F1^5F1$ (*10*). The largest chemical shift changes in $^4F1$ occur for residues in the D−E loop and in strand E. The overall pattern of chemical shift changes for residues in $^5F1$ is quite different, and most of the significant changes occur for residues close to $^4F1$. For example, strands A′ and B′ and the B′−C′ and D′−E′ loops in $^5F1$ all contribute to the intermodule interface in the uncomplexed module pair (*10*); these regions all exhibit significant chemical shift changes. However, not all significant changes in $^5F1$ are observed for residues close to the interface; for example, the largest ^{15}N or H^N chemical shift change in $^5F1$ is for Cys88.

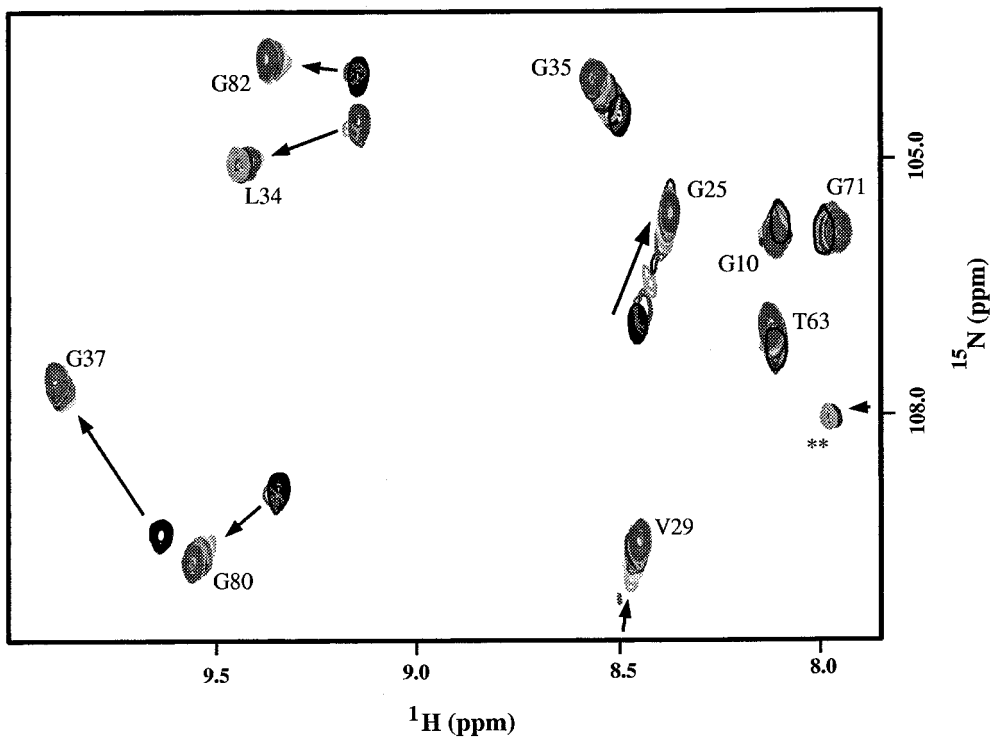

FIGURE 2: Overlay of a region of two-dimensional $^{15}N-^{1}H$ HSQC spectra (recorded at a ^{1}H frequency of 600 MHz) of $^{4}F1^{5}F1$ for a range of $^{4}F1^{5}F1$:$D3_{17-37}$ ratios at pH 5.5 and 37 °C. The HSQC spectra were recorded at $^{4}F1^{5}F1$:$D3_{17-37}$ ratios of 1:0, 1:0.3, 1:0.5, 1:0.8, 1:1.1, 1:1.4, 1:1.8, 1:2, 1:3, 1:4, and 1:8. The arrows indicate the direction of the chemical shift changes on addition of $D3_{17-37}$. The peak labeled with two asterisks (**) arises from an unassigned arginine side chain Hϵ; this peak and Leu34 are aliased in the ^{15}N dimension.

$^{13}C-^{1}H$ HSQC spectra of [*u*-$^{13}C^{15}N$]$^{4}F1^{5}F1$ were recorded in the absence and presence of $D3_{7-38}$ to measure chemical shift changes of side chain methyl groups of $^{4}F1^{5}F1$. Chemical shift assignments were obtained using three-dimensional spectra as described in Materials and Methods. Methyl groups of Ile41, Thr32, and Val14 remained unassigned in the complex due to spectral overlap and broadening. The three residues (Leu34, Thr42, and Thr44) whose $^{13}C_{\gamma}H_3$ or $^{13}C_{\delta}H_3$ chemical shifts undergo the largest changes are shown in blue in Figure 4.

From Figure 4, it is clear that the large majority of chemical shift changes occur on one face of the $^{4}F1^{5}F1$ structure. The changes in chemical shifts of the side chain methyl $^{13}CH_3$ groups of residues Leu34, Thr42, and Thr44 suggest the involvement of hydrophobic interactions in peptide binding. This is consistent with previous work showing that electrostatic interactions do not play a dominant role in the binding of the N-terminal domain of fibronectin to immobilized D peptides from *S. aureus* (*8*). In addition, sequence alignments of fibronectin binding peptides from FnBPA of *S. aureus* and FnBA of *St. dysgalactiae* showed that hydrophobic residues are conserved in two positions in the C-terminal region of each repeat (*13*). Negatively charged residues in $D3_{17-37}$ do, however, also appear to play a role in fibronectin binding (*11*), so it is interesting to note that an unassigned arginine side chain H$^{\epsilon}$ resonance is shifted significantly downfield in the HSQC spectrum of peptide-bound $^{4}F1^{5}F1$ (see Figure 2). In addition, both Arg40, in the D−E loop of $^{4}F1$, and Arg48, in the A′-strand of $^{5}F1$ and close to the intermodule interface (*10*), undergo large (>0.5 ppm) combined backbone chemical shift changes on peptide binding (Figure 3A). Thus, the $^{4}F1^{5}F1$ chemical shift changes upon peptide binding suggest the involvement of both hydrophobic and electrostatic interactions. The unfolded nature of D1−D4 results in both polar and hydrophobic groups in the protein being exposed and accessible for binding (*12*).

NOEs between all the adjacent strands of the four β-sheets that are observed in free $^{4}F1^{5}F1$ can be assigned in the three-dimensional NOESY-HSQC spectrum of peptide-bound $^{4}F1^{5}F1$. Furthermore, no new protein−protein NOEs could be assigned in the three-dimensional ^{15}N NOESY-HSQC spectrum of the [*u*-^{15}N]$^{4}F1^{5}F1-D3_{17-37}$ complex at pH 5.5 that had not been previously observed in free $^{4}F1^{5}F1$ at pH 4.5 (*18*). These results indicate that the overall secondary structure remains intact in the free and peptide-bound forms of $^{4}F1^{5}F1$. However, changes in the relative orientation of the two modules when bound to D3 cannot be ruled out. No NOEs between protons in the peptide and the protein can be assigned in the three-dimensional NOESY-HSQC spectrum of peptide-bound $^{4}F1^{5}F1$, although such NOEs may not be seen due to exchange broadening for cross-peaks of residues close to the binding site in $^{4}F1^{5}F1$.

Interaction of D1−D4 with $^{4}F1^{5}F1$. To identify the residues from D1−D4 that are involved in binding to $^{4}F1^{5}F1$, two-dimensional $^{15}N-^{1}H$ HSQC spectra of [*u*-^{15}N]D1−D4 were recorded in the absence and presence of unlabeled $^{4}F1^{5}F1$. Parts of the backbone amide region of HSQC spectra of D1−D4 in the absence and presence of $^{4}F1^{5}F1$ are shown in Figure 5A. The spectrum of D1−D4 in the presence of $^{4}F1^{5}F1$ has a number of significantly less intense cross-peaks compared to the spectrum of free D1−D4, although no changes in chemical shift are apparent between the spectra. The reduction in peak intensity is likely to be a result of both chemical exchange effects and the increase in molecular weight on complex formation and, therefore, the longer

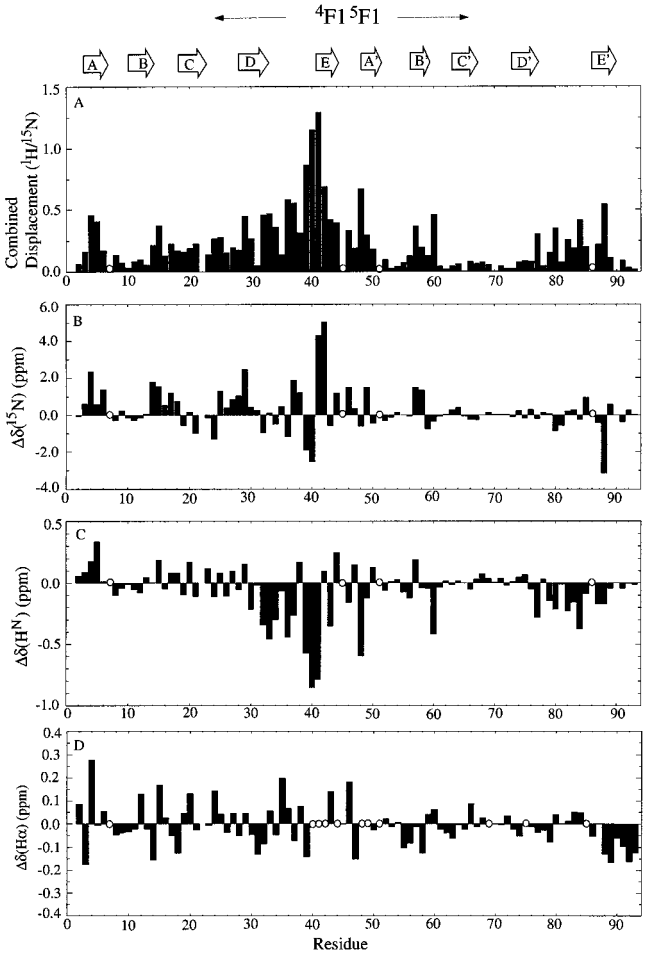

FIGURE 3: Backbone chemical shift changes of ^{4}F1^{5}F1 upon binding of D3$_{17-37}$ ($\Delta\delta = \delta^{free} - \delta^{bound}$). (A) Magnitude of combined backbone amide ^{15}N and ^{1}H (H^N) chemical shift changes ($=\delta^{15}N/8.5 + \delta H^N$; for glycine residues $= \delta^{15}N/6.5 + \delta H^N$). (B) Change in the backbone amide ^{15}N shift. (C) Change in the backbone amide ^{1}H shift. (D) Change in the H$^\alpha$ shift. An open circle indicates residues for which data were not obtained. The ^{4}F1^{5}F1 secondary structure is indicated at the top of the figure.

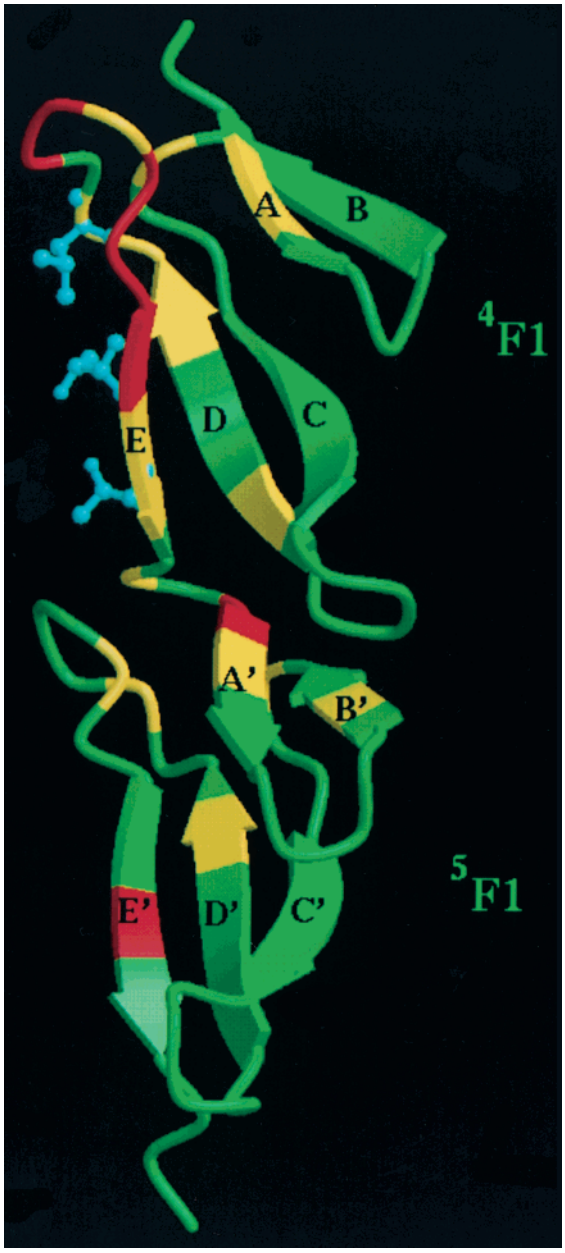

FIGURE 4: Ribbon diagram of uncomplexed ^{4}F1^{5}F1 (*10*) with combined ^{15}N and H^N chemical shift changes (Figure 3A). Residues with chemical shift changes of $\geq$0.3 and $\geq$0.5 ppm are shown in yellow and red, respectively. Side chain heavy atoms of Leu34, Thr42, and Thr44 are shown in cyan. All other residues are shown in green. The diagram was prepared using MolScript2 (*44*) and Raster3D (*45*). β-Strands of ^{4}F1^{5}F1 (*18*) are labeled.

overall correlation time. As D1, D2, and D3 have been shown to bind ^{4}F1^{5}F1 (*8*), there may be more than one molecule of ^{4}F1^{5}F1 bound to each D1−D4 molecule, further increasing the size of the complex. No new resonances corresponding to D1−D4 bound to ^{4}F1^{5}F1 were observed.

The changes to D1−D4 peak intensities have been quantified (called I_b) as the ratio of the bound peak intensity to the free peak intensity (Figure 5B). I_b has been normalized so that the most N-terminal residue observed in the spectrum (Gln2) takes the value of 1; this normalization is required to account for slight differences in the conditions under which the HSQC spectra were recorded (primarily from differences in the concentration of D1−D4 after ^{4}F1^{5}F1 was added). The largest decreases in intensity occur for peaks from residues in the C-terminal halves of D1, D2, and D3. If a lower I_b value can be interpreted as resulting from a higher-affinity binding to ^{4}F1^{5}F1, then the low I_b values observed for D3 are consistent with previous studies where it was found that D3 binds with higher affinity to fibronectin than D1 or D2 (*8*, *13*, *38*). In addition, the low I_b values for residues in the C-terminal halves of the D repeats agree with previous studies where it was found that the C-terminal halves of the D repeats were the primary fibronectin-binding sites in D1−D4 (*8*, *11*).

I_b Values for D3$_{7-38}$. Figure 6 shows I_b values for D3$_{7-38}$ at a range of D3$_{7-38}$:^{4}F1^{5}F1 ratios measured in ^{15}N-filtered TOCSY spectra. The spectra were normalized using the intensity of the appropriate cross-peak in a normal TOCSY spectrum of D3$_{7-38}$. The intensity of the peak for Ile8 (Ile84 in D1−D4) is normalized to 1 in each spectrum to account for small differences in the D3$_{7-38}$ concentration. These data illustrate that the residues of the D3 repeat that appear to be involved in binding ^{4}F1^{5}F1 are similar in D1−D4 and D3$_{7-38}$. The main difference that is observed is for residue 95 which is one of two residues which differs between the two sequences. In FnBP variant C (D1−D4 sequence), this

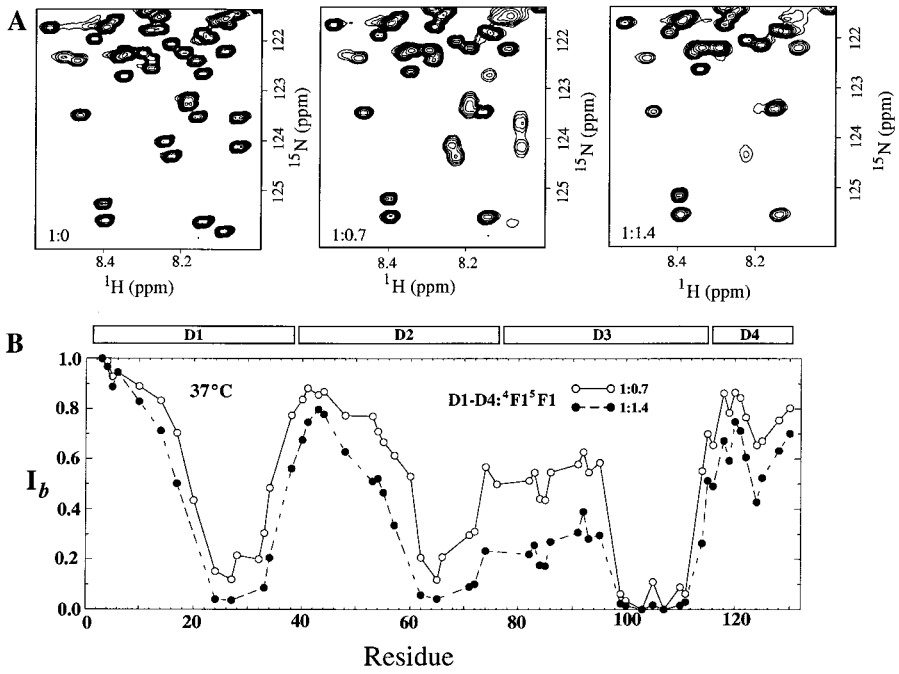

FIGURE 5: (A) Region of two-dimensional ^{15}N−^{1}H HSQC spectra (recorded at a ^{1}H frequency of 500 MHz) of D1−D4 at D1−D4:^{4}F1^{5}F1 ratios of approximately 1:0, 1:0.7, and 1:1.4 at 37 °C. The residues for unlabeled ^{4}F1^{5}F1 were eliminated using isotope filtering. (B) I_b values for D1−D4 at D1−D4:^{4}F1^{5}F1 ratios of 1:0.7 (○) and 1:1.4 (●) at 37 °C.

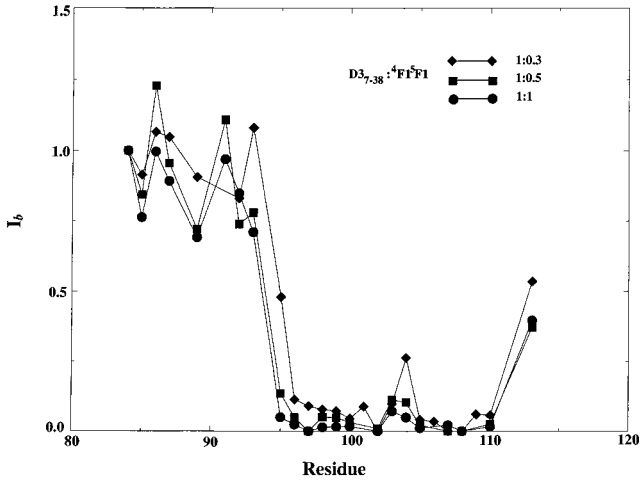

FIGURE 6: I_b values for $D3_{7-38}$ at $D3_{7-38}$:^{4}F1^{5}F1 ratios of approximately 1:0.3 (◆), 1:0.5 (■), and 1:1 (●). The residues are numbered according to the corresponding residue numbers in D1−D4.

residue is an asparagine, while in FnBPA ($D3_{7-38}$ sequence), this residue is a serine (*12*).

CONCLUSIONS

The results presented here indicate the residues in ^{4}F1^{5}F1 which are involved in binding to the D3 repeat of FnBPA of the pathogenic bacteria *S. aureus*. The chemical shift changes that occur in ^{4}F1^{5}F1 upon peptide binding suggest that the binding site for $D3_{17-37}$ is located on one face of ^{4}F1^{5}F1, and primarily on the D−E loop and E strand of ^{4}F1, although other residues in ^{4}F1 and ^{5}F1 may also be involved. Both hydrophobic and electrostatic interactions appear to be involved. In a recent study (*14*), a GST fusion protein containing D1−D4 was able to bind ^{2}F1^{3}F1 and ^{4}F1^{5}F1 and a synthetic D3 peptide bound ^{1}F1^{2}F1 and ^{2}F1^{3}F1, albeit more weakly than ^{4}F1^{5}F1. In view of the degree of sequence identity between ^{2}F1^{3}F1 and ^{4}F1^{5}F1 (∼40%), D3 may bind ^{2}F1^{3}F1 like it binds ^{4}F1^{5}F1.

In the case of the fibronectin binding protein, residues in the C-terminal region of the D repeats (D1, D2, and D3) are involved in the interaction, and the polypeptide chain appears to become more ordered upon binding to ^{4}F1^{5}F1.

A number of systems have been identified where a protein exists in a highly unfolded state under physiological conditions but adopts a more ordered conformation when complexed with its target protein (*39*). In some cases, substantial disorder-to-order transitions have been observed. For example, upon binding to the KIX domain of the coactivator CBP, the unfolded phosphorylated kinase-inducible domain of CREB folds into a conformation containing two α-helices, one of which interacts with a hydrophobic groove on KIX (*40*). For D1−D4, the changes upon binding to ^{4}F1^{5}F1 may be much less extensive. Indeed, there appears to be little change in the conformational properties of the N-terminal halves of each of the D repeats. Similar behavior has been observed for the interaction of the flagellum specific sigma factor σ28 with its inhibitor FlgM, where approximately 50% of the FlgM residues remain unstructured on complex formation (*41*).

The definitive answer to the question of how D3 binds to ^{4}F1^{5}F1 would require the determination of the structure of the ^{4}F1^{5}F1−$D3_{17-37}$ complex. Although this work is ongoing, the lack of peptide−protein NOEs in the three-dimensional NOESY-HSQC spectrum of ^{4}F1^{5}F1−$D3_{17-37}$ and the low intensity of peaks arising from residues in bound $D3_{17-37}$ (Figure 1) make this challenging. However, with the proposed adoption of more extended conformations by residues at the C-terminus of D3, it is tempting to speculate that an additional strand, formed by residues in $D3_{17-37}$, docks alongside strand E of ^{4}F1. Peptide binding by formation of an additional β-strand in a β-sheet present in

the uncomplexed protein has been observed for other proteins (*42*, *43*).

A synergistic effect has been observed when multiple D repeats from D1−D4 are involved in binding to fibronectin fragments. For example, Huff et al. (*8*) found that D1−D4 binds about two molecules of the N-terminal domain of fibronectin with an affinity that exceeds that for the isolated D repeats by a factor of 1000 or more and that D1−D4 binds to $^4F1^5F1$, with about 10- or 20-fold higher affinity than $D3_{17-37}$. Thus, it has been suggested previously that the interaction between FnBPA and fibronectin may involve more than one site on each of the molecules (*16*). As fibronectin is in an insoluble fibrillar form in the extracellular matrix, it is also possible that multiple fibronectin binding sites in D1−D4 enable the bacteria to take advantage of this relatively high concentration of fibronectin.

ACKNOWLEDGMENT

We thank Dr. Robin Aplin for mass spectrometry, Dr. Maureen Pitkeathly for peptide synthesis, and Dr. Richard Smith for providing D1−D4 and for helpful discussions.

REFERENCES

1. Patti, J. M., and Höök, M. (1994) *Curr. Opin. Cell Biol. 6*, 752−758.
2. Patti, J. M., Allen, B. L., McGavin, M. J., and Höök, M. (1994) *Annu. Rev. Microbiol. 48*, 585−617.
3. Kuusela, P. (1978) *Nature 276*, 718−720.
4. Bork, P., Downing, A. K., Kieffer, B., and Campbell, I. D. (1996) *Q. Rev. Biophys. 29*, 119−167.
5. Mosher, D. F., and Proctor, R. A. (1980) *Science 209*, 927−929.
6. Bozzini, S., Visai, L., Pignatti, P., Peterson, T. E., and Speziale, P. (1992) *Eur. J. Biochem. 207*, 327−333.
7. Sakata, N., Jakab, E., and Wadström, T. (1994) *J. Biochem. 115*, 843−848.
8. Huff, S., Matsuka, Y. V., McGavin, M. J., and Ingham, K. C. (1994) *J. Biol. Chem. 269*, 15563−15570.
9. Matsuka, Y. V., Medved, L. V., Brew, S. A., and Ingham, K. C. (1994) *J. Biol. Chem. 269*, 9539−9546.
10. Williams, M. J., Phan, I., Harvey, T. S., Rostagno, A., Gold, L. I., and Campbell, I. D. (1994) *J. Mol. Biol. 235*, 1302−1311.
11. McGavin, M. J., Raucci, G., Gurusiddappa, S., and Höök, M. (1991) *J. Biol. Chem. 266*, 8343−8347.
12. Penkett, C. J., Redfield, C., Jones, J. A., Dodd, I., Hubbard, J., Smith, R. A. G., Smith, L. J., and Dobson, C. M. (1998) *Biochemistry 37*, 17054−17067.
13. McGavin, M. J., Gurusiddappa, S., Lindgren, P.-E., Lindberg, M., Raucci, G., and Höök, M. (1993) *J. Biol. Chem. 268*, 23946−23953.
14. Joh, D., Speziale, P., Gurusiddappa, S., Manor, J., and Höök, M. (1998) *Eur. J. Biochem. 258*, 897−905.
15. Potts, J. R., Bright, J. R., Bolton, D., Pickford, A. R., and Campbell, I. D. (1999) *Biochemistry 38*, 8304−8312.
16. House-Pompeo, K., Xu, Y., Joh, D., Speziale, P., and Höök, M. (1996) *J. Biol. Chem. 271*, 1379−1384.
17. Penkett, C. J., Redfield, C., Dodd, I., Hubbard, J., McBay, D. L., Mossakowska, D. E., Smith, R. A. G., Dobson, C. M., and Smith, L. J. (1997) *J. Mol. Biol. 274*, 152−159.
18. Williams, M. J., Phan, I., Baron, M., Driscoll, P. C., and Campbell, I. D. (1993) *Biochemistry 32*, 7388−7395.
19. Williams, M. J., and Campbell, I. D. (1994) *Methods Enzymol. 245*, 451−469.
20. Pickford, A. R., Potts, J. R., Bright, J. R., Phan, I., and Campbell, I. D. (1997) *Structure 5*, 359−370.
21. Bright, J. R., Pickford, A. R., Potts, J. R., and Campbell, I. D. (2000) in *Methods in Molecular Biology*, Humana Press Inc., Totowa, NJ (in press).
22. Soffe, N., Boyd, J., and Leonard, M. (1995) *J. Magn. Reson., Ser. A 116*, 117−121.
23. Bodenhausen, G., and Ruben, D. J. (1980) *Chem. Phys. Lett. 69*, 185−189.
24. Jeener, J., Meier, B. H., Bachmann, P., and Ernst, R. R. (1979) *J. Chem. Phys. 71*, 4546−4553.
25. Kumar, A., Ernst, R. R., and Wüthrich, K. (1980) *Biochem. Biophys. Res. Commun. 95*, 1−6.
26. Macura, S., and Ernst, R. R. (1980) *Mol. Phys. 41*, 95−117.
27. Kay, L. E., Marion, D., and Bax, A. (1989) *J. Magn. Reson. 84*, 72−84.
28. Marion, D., Driscoll, P. C., Kay, L. E., Wingfield, P. T., Bax, A., Gronenborn, A. M., and Clore, G. M. (1989) *Biochemistry 28*, 6150−6156.
29. Marion, D., Kay, L. E., Sparks, S. W., Torchia, D. A., and Bax, A. (1989) *J. Am. Chem. Soc. 111*, 1515−1517.
30. Otting, G., and Wüthrich, K. (1989) *J. Magn. Reson. 85*, 586−594.
31. Hwang, T.-L., and Shaka, A. J. (1995) *J. Magn. Reson., Ser. A 112*, 275−279.
32. Phan, I. Q. H., Boyd, J., and Campbell, I. D. (1996) *J. Biomol. NMR 8*, 369−378.
33. Santoro, J., and King, G. C. (1992) *J. Magn. Reson. 97*, 202−207.
34. Vuister, G. W., and Bax, A. (1992) *J. Magn. Reson. 98*, 428−435.
35. Grzesiek, S., and Bax, A. (1992) *J. Am. Chem. Soc. 114*, 6291−6293.
36. Logan, T. M., Olejniczak, E. T., Xu, R. X., and Fesik, S. W. (1993) *J. Biomol. NMR 3*, 225−231.
37. Wishart, D. S., Sykes, B. D., and Richards, F. M. (1991) *J. Mol. Biol. 222*, 311−333.
38. Raja, R. H., Raucci, G., and Höök, M. (1990) *Infect. Immun. 58*, 2593−2598.
39. Plaxco, K. W., and Gross, M. (1997) *Nature 386*, 657−658.
40. Radhakrishnan, I., Perez-Alvarado, G. C., Parker, D., Dyson, H. J., Montminy, M. R., and Wright, P. E. (1997) *Cell 91*, 741−752.
41. Daughdrill, G. W., Chadsey, M. S., Karlinsey, J. E., Hughes, K. T., and Dahlquist, F. W. (1997) *Nat. Struct. Biol. 4*, 285−291.
42. Kuehn, M. J., Kihlberg, J., Slonim, L. N., Flemmer, K., Bergfors, T., and Hultgren, S. J. (1993) *Science 262*, 1234−1241.
43. Mott, H. R., Owen, D., Nietlispach, D., Lowe, P. N., Manser, E., Lim, L., and Laue, E. (1999) *Nature 399*, 384−388.
44. Kraulis, P. (1991) *J. Appl. Crystallogr. 24*, 946−950.
45. Merritt, E. A., and Murphy, M. E. P. (1994) *Acta Crystallogr. D50*, 869−873.

BI992267K